Supporting Information

Unhavaithaya and Orr-Weaver 10.1073/pnas.1320074110

SI Materials and Methods

Ovary Fixation and Immunostaining. Ovaries from 2- to 3-d-old yeast-fed females were dissected in cold PBS [137 mM NaCl, 2.7 mM KCl, 10 mM Na_2HPO_4, 2 mM KH_2PO_4 (pH 7.4)] and fixed in 4% (wt/vol) paraformaldehyde and 0.5% (vol/vol) Nonidet P-40 in PBS/heptane (1:3) for 20 min. After rinsing with 0.2% (vol/vol) Tween-20 in PBS (PBST), ovaries were separated by teasing apart with forceps and washed with PBST for 10 min three times. The samples were blocked in 1% (wt/vol) BSA in PBST for at least 1 h and incubated with primary antibodies overnight at 4 °C.

Ovary Immunoblots. Groups of 30 ovary pairs were homogenized in 250 μL of ice-cold homogenization buffer [50 mM Tris·HCl (pH 8.0), 150 mM NaCl, 1% (vol/vol) Triton X-100, 1× EDTA-free protease inhibitor mixture (Roche)]. The lysates were centrifuged for 10 min at 16,000 × *g*, and the supernatant was subjected to SDS/PAGE. Western blotting was carried out as described in the study by Pesin and Orr-Weaver (1). Antibodies used were rabbit anti-CAL1 (Aaron Straight, Stanford University School of Medicine, Stanford, CA) at 1:2,000, rabbit anti–CENP-C (Christian Lehner, University of Zurich, Zurich, Switzerland) at 1:5,000, and rat antitubulin (Harlan Sera-Lab) at 1:200. The signal was detected with HRP-conjugated secondary antibodies using Pierce ECL Plus Western Blotting substrate.

Quantification of CID Staining. CID fluorescence intensity was quantified from region 3 oocytes on images acquired on a Zeiss LSM 700 confocal microscope using a modification of the protocol of Lidsky et al. (2). Quantifications were performed on the sum projections of Z stacks, using ImageJ software (National Institutes of Health). To determine the CID signal region, a circle that circumscribed all the CID foci was identified by applying a manually adjusted threshold. A larger concentric circle with twofold the diameter of the smaller CID signal region was selected for subsequent background correction. To determine the background value of the CID signal region, average integrated pixel intensity per unit area between the smaller circle and the larger circle was determined, and later used for background correction to obtain the final total pixel intensity of the CID signal region.

1. Pesin JA, Orr-Weaver TL (2007) Developmental role and regulation of cortex, a meiosis-specific anaphase-promoting complex/cyclosome activator. *PLoS Genet* 3(11):e202.

2. Lidsky PV, Sprenger F, Lehner CF (2013) Distinct modes of centromere protein dynamics during cell cycle progression in Drosophila S2R+ cells. *J Cell Sci* 126(Pt 20):4782–4793.

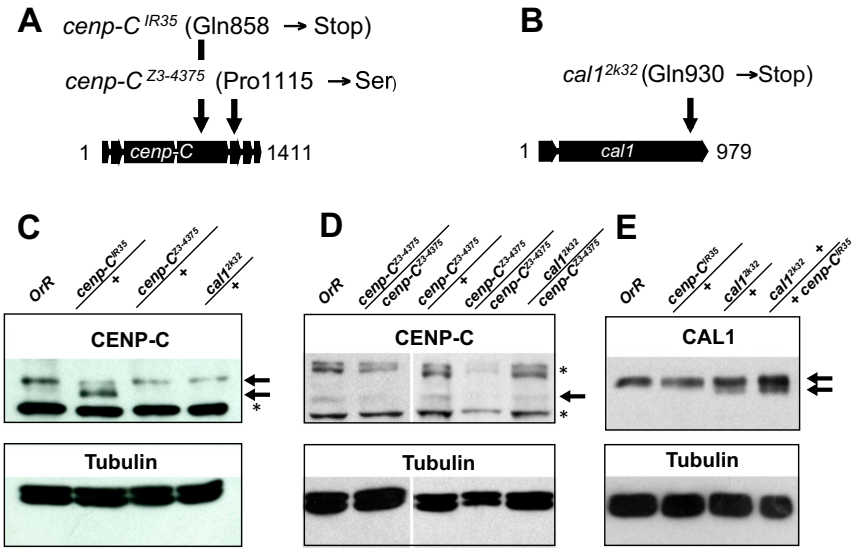

Fig. S1. *cal1* and *cenp-C* centromere protein mutants. (*A*) Positions and changes of the nonsense mutation in *cenp-C*^{IR35} and the missense mutation in *cenp-C*$^{Z3\text{-}4375}$ are indicated by the arrows. Exons are designated by black arrows in the diagram. (*B*) Change of Gln930 to a stop codon in *cal1*^{2k32} is indicated by the arrow in the diagram. (*C*) Western blot of ovary extracts from flies of the indicated genotypes probed with anti–CENP-C antibody. The truncated form of CENP-C resulting from the *cenp-C*^{IR35} stop codon is visible, whereas *cenp-C*$^{Z3\text{-}4375}$ produces a full-length polypeptide (arrows). The asterisk indicates a cross-reacting band. (*D*) *cenp-C*$^{Z3\text{-}4375}$ mutation destabilizes the protein to cause decreased levels (arrow). The asterisks indicate cross-reacting bands. (*E*) Western blot of ovary extracts from the indicated genotypes probed with anti-CAL1. A truncated protein is produced by the *cal1*^{2K32} mutation (arrows). Tubulin serves as a loading control for all Western blots. CAL1, chromosome alignment 1; CENP-C, centromere protein-C; OrR, OregonR.

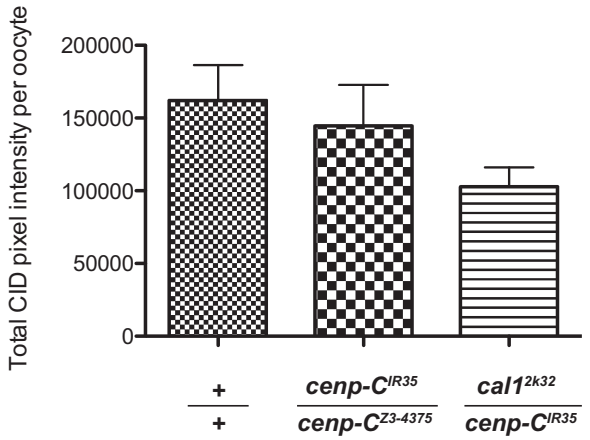

Fig. S2. Quantification of CID immunofluorescence staining. A graph of average values of CID foci intensity summed over each of seven nuclei for WT, *cenp-C*$^{Z3\text{-}4375}$/*cenp-C*^{IR35}, and *cal1*^{2k32} +/+ *cenp-C*^{IR35} late region 3 oocyte nuclei is shown. The levels of CID staining are not significantly different in the mutants from WT by a two-tailed *t* test (*cenp-C*$^{Z3\text{-}4375}$/*cenp-C*^{IR35}, $P = 0.74$; *cal1*^{2k32} +/+ *cenp-C*^{IR35}, $P = 0.06$). The error bars show the SEM.

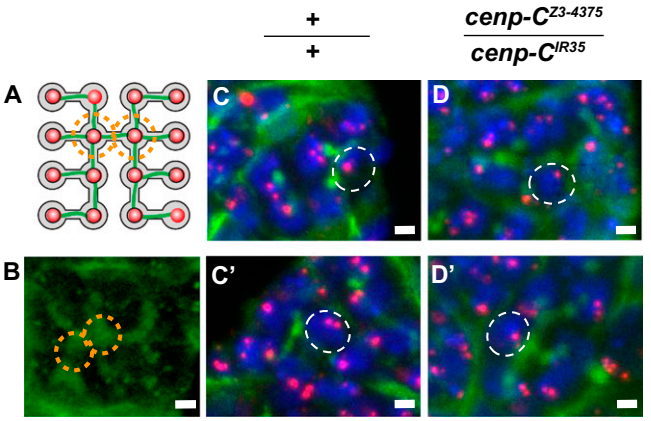

Fig. S3. Initiation of centromere clustering occurs normally in *cenp-C*$^{Z3\text{-}4375}$/*cenp-C*^{IR35}. (*A*) Diagram of the 16 cell cysts, cytoplasmic bridges, and connecting fusome. The two pro-oocytes (orange dotted circles) are distinguishable because they each have four fusome branches, shown by immunofluorescence staining in *B*. The more posterior of these two cells becomes the oocyte by region 3 of the germaria. (*C* and *C*′) CID (red), IB1 fusome (green), and DAPI (blue) staining of two region 2a germaria of WT *Oregon R*. (*D* and *D*′) Same staining for two *cenp-C*$^{Z3\text{-}4375}$/*cenp-C*^{IR35} germaria. The pro-oocyte nucleus is outlined by the white dotted line. One to two CID foci are observed in the pro-oocytes of both strains. (Scale bars, 2 μm.) Micrographs were taken with a Zeiss LSM710 confocal microscope. Eleven cysts were scored for the *cenp-C* mutant, and 7 were scored for the WT control. The number of foci in the two pro-oocytes for the *cenp-C* mutant cysts were as follows: 1,2; 1,1; 2,2; 2,2; 1,2; 1,2; 1,2; 1,2; 2,2; 1,1; and 1,2. The number of foci in the two pro-oocytes for the WT cysts were as follows: 1,1; 1,2; 1,2; 1,2; 1,2; 1,2; and 1,2.

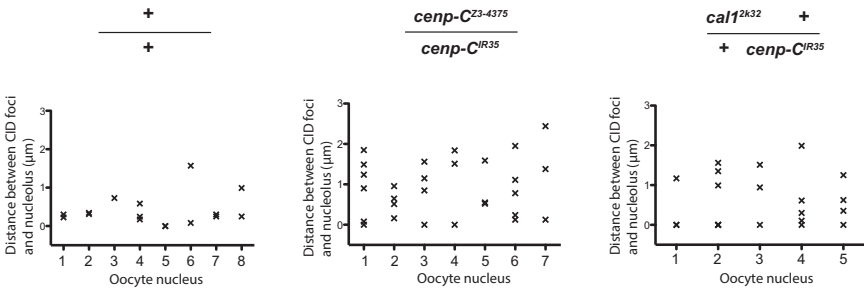

Fig. S4. Quantification of the distance between CID foci and the nucleolus. A scatterplot shows the distance between CID foci and the nucleolus (*y* axis; measured in micrometers) in individual oocytes (*x* axis; each number represents an individual oocyte) of indicated genotypes. The centromere protein mutants not only have increased numbers of CID foci but these are not associated with the nucleolus. By the Wilcoxon rank sum test, the number of foci separate from the nucleolus (>0 μm) in the mutants is significantly different from WT (*cenp-C*$^{Z3\text{-}4375}$/*cenp-C*^{IR35}, $P = 0.01$; *cal1*^{2k32} +/+ *cenp-C*^{IR35}, $P = 0.03$).

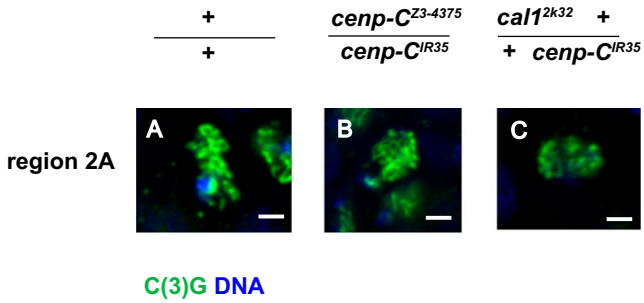

Fig. S5. Synaptonemal complex (SC) assembles normally in centromere protein mutants. Representative C(3)G (green) and DAPI (blue) staining in a pro-oocyte nucleus from region 2A of WT, *cenp-C$^{Z3\text{-}4375}$/cenp-C^{IR35}*, and *cal1^{2k32} +/+ cenp-C^{IR35}* mutants is shown. The SC assembles into normal ribbon structures in region 2A of the mutants. The number of germaria scored for SC assembly was 36 for WT, 32 for *cenp-C$^{Z3\text{-}4375}$/cenp-C^{IR35}*, and 33 for *cal1^{2K32} +/+ cenp-C^{IR35}*. (Scale bars, 2 μm.) Micrographs were taken with a Nikon Eclipse Ti microscope.

Table S1. Nondisjunction tests of centromere protein mutant females with rescuing transgenes

Female genotype	*cal1^{2k32} +/+ cenpC^{IR35}*	[*cal1::gfp*]/+; *cal1^{2k32} +/+ cenp-C^{IR35}*	[*cal1::gfp*]/[*cal1::gfp*]; *cal1^{2k32} +/+ cenp-C^{IR35}*	[*yfp::cenpC*]/+; *cal1^{2k32} +/+ cenp-C^{IR35}*	[*yfp::cenpC*]/[*yfp::cenpC*]; *cal1^{2k32} +/+ cenp-C^{IR35}*
Ova					
X; 4	155	710	932	717	1,056
X; 0	1	1	6	14	0
X; 44	2	0	0	0	0
0; 4	8	12	8	14	6
0; 0	1	1	0	3	0
0; 44	0	0	0	0	0
XX; 4	5	13	11	14	1
XX; 0	0	1	1	0	0
XX; 44	0	0	0	0	0
Total progeny	172	738	958	762	1,063
Adjusted total	186	765	978	793	1,070
X exceptions, %	**15.3**	**7.1***	**4.1†**	**7.9**	**1.3‡**
4 exceptions, %	**2.3**	**0.4**	**0.7**	**2.2**	**0**

Total percent *X* and *4th* nondisjunction is shown in bold.
*Significantly different from *cal1^{2K32} +/+ cenpC^{IR35}* without rescue transgene by the *X* nondisjunction significance test of Zeng et al. (1); $P = 0.05$.
†Significantly different from *cal1^{2K32} +/+ cenpC^{IR35}* without rescue transgene by the *X* nondisjunction significance test of Zeng et al. (1); $P = 0.006$.
‡Significantly different from *cal1^{2K32} +/+ cenpC^{IR35}* without rescue transgene by the *X* nondisjunction significance test of Zeng et al. (1); $P < 1.0e\text{-}04$.

1. Zeng Y, Li H, Schweppe NM, Hawley RS, Gilliland WD (2010) Statistical analysis of nondisjunction assays in Drosophila. *Genetics* 186(2):505–513.

Table S2. Nondisjunction tests for centromere protein mutants over deficiencies

Female genotype	*cal1^{2K32} +/+ Df cenp-C^{1}**	*Df cal1^{2†} +/+ cenp-C^{IR35}*
Ova		
X	405	434
0	1	0
XX	0	0
Total progeny	406	434
Adjusted total	407	434
X exceptions, %	**0.5**	**0**

Total percent *X* nondisjunction is shown in bold. *Df*, deficiency.
**Df(3R)Exel6149*.
†*Df(3R)Exel6176*.

Table S3. Nondisjunction test for centromere protein mutant males

Male genotype	+/+	*cal1*^{2K32} +/+ *cenp-C*^{IR35}
Sperm		
X	439	71
Y(Y)	724	175
0	3	1
XY(Y)	1	0
XX	0	2
XXY(Y)	0	0
Total progeny	1,167	249
Nullo *XY*, %	0.25	0.4
XY(Y), %	0.08	0
XX, %	0	0.8
XXY(Y), %	0	0
Total nondisjunction, %	**0.33**	**1.2**

Total percent *X* and *Y* nondisjunction is shown in bold.